Identification of the Dominant Precession-Damping Mechanism in Fe, Co, and Ni by First-Principles Calculations

K. Gilmore,[1,2] Y. U. Idzerda,[2] and M. D. Stiles[1]
[1]National Institute of Standards and Technology, Gaithersburg, Maryland 20899-8412, USA
[2]Physics Department, Montana State University, Bozeman, Montana 59717, USA
(Received 4 May 2007; published 9 July 2007)

The Landau-Lifshitz equation reliably describes magnetization dynamics using a phenomenological treatment of damping. This Letter presents first-principles calculations of the damping parameters for Fe, Co, and Ni that quantitatively agree with existing ferromagnetic resonance measurements. This agreement establishes the dominant damping mechanism for these systems and takes a significant step toward predicting and tailoring the damping constants of new materials.

DOI: 10.1103/PhysRevLett.99.027204 PACS numbers: 75.40.Gb, 76.60.Es

Magnetic damping determines the performance of magnetic devices including hard drives, magnetic random access memories, magnetic logic devices, and magnetic field sensors. The behavior of these devices can be modeled using the Landau-Lifshitz (LL) equation [1]

$$\dot{\mathbf{m}} = -|\gamma|\mathbf{m} \times \mathbf{H}_{\text{eff}} - \frac{\lambda}{m^2}\mathbf{m} \times (\mathbf{m} \times \mathbf{H}_{\text{eff}}), \quad (1)$$

or the essentially equivalent Gilbert (LLG) form [2,3]. The first term describes precession of the magnetization $\mathbf{m}$ about the effective field $\mathbf{H}_{\text{eff}}$, where $\gamma = g\mu_0\mu_B/\hbar$ is the gyromagnetic ratio. The second term is a phenomenological treatment of damping with the adjustable rate λ. The Gilbert form replaces this term with $\alpha\hat{m} \times \dot{\mathbf{m}}$ using the dimensionless damping constant $\alpha = \lambda/\gamma m$. The LL(G) equation adequately describes dynamics measured by techniques as varied as ferromagnetic resonance (FMR) [4], magneto-optical Kerr effect [5], x-ray absorption spectroscopy [6], and spin-current driven rotation with the addition of a spin-torque term [7,8].

Access to a range of damping rates in metallic materials is desirable when constructing devices for different applications. Empirically, doping NiFe alloys with transition metals [9] or rare earths [10] has produced compounds with damping rates in the range of $\alpha = 0.01$ to 0.8. A recent investigation of adding vanadium to iron resulted in an alloy with a decreased damping rate [11]. Unfortunately, the damping rate of a new material cannot be predicted because there has not yet been a first-principles calculation of damping that quantitatively agrees with experiment. The challenging pursuit of new materials with specific or lowered damping rates is further complicated by the expectation that, as device size continues to be scaled down, material parameters, such as λ, should change [12]. A detailed understanding of the important damping mechanisms in metallic ferromagnets and the ability to predictively calculate damping rates would greatly facilitate the design of new materials appropriate for a variety of applications.

The temperature dependence of damping in the transition metals has been carefully characterized through measurement of small angle dynamics by FMR [13,14]. While one might naïvely expect damping to increase monotonically with temperature, as it does for Fe, both Co and Ni also exhibit a dramatic rise in damping at low temperature as the temperature decreases. These observations indicate that two primary mechanisms are involved. Subsequent experiments [15,16] partition these nonmonotonic damping curves into a *conductivitylike* term that decreases with temperature like the conductivity and a *resistivitylike* term that increases with temperature like the resistivity. The two terms were found to give nearly equal weight to the damping curve of Ni.

A number of mechanisms for damping in these systems have been proposed [14,17–24]. See the review by Heinrich [25] for a more complete discussion. However, none of the models have been shown to quantitatively agree with measured values. The torque-correlation model of Kambersky [17] qualitatively matches the data, but has not been quantitatively evaluated in a rigorous fashion. Here, we report first-principles calculations of the Landau-Lifshitz damping constant according to Kambersky's torque-correlation expression. Quantitative comparison of the present calculations to the measured FMR values [13] positively identifies this damping pathway as the dominant effect in the transition metal systems. In addition to presenting these primary conclusions, we also describe the relationship between the torque-correlation model and the more widely understood breathing Fermi surface model [18,21], showing that the results of both models agree quantitatively in the low scattering rate limit.

The breathing Fermi surface model of Kambersky predicts

$$\lambda = \frac{g^2\mu_B^2}{\hbar}\sum_n \int \frac{dk^3}{(2\pi)^3}\,\eta(\epsilon_{n,k})\left(\frac{\partial\epsilon_{n,k}}{\partial\theta}\right)^2\frac{\tau}{\hbar}. \quad (2)$$

This model offers a qualitative explanation for the low temperature conductivitylike contribution to the measured

damping. The model describes damping of uniform precession as due to variations $\partial\epsilon_{n,k}/\partial\theta$ in the energies $\epsilon_{n,k}$ of the single-particle states with respect to the spin direction θ. The states are labeled with a wave vector k and band index n. As the magnetization precesses, the spin-orbit interaction changes the energy of the electronic states, pushing some occupied states above the Fermi level and some unoccupied states below the Fermi level. Thus, electron-hole pairs are generated near the Fermi level even in the absence of changes in the electronic populations. The η function in Eq. (2) is the negative derivative of the Fermi function and picks out only states near the Fermi level to contribute to the damping. g is the Landé g factor and μ_B is the Bohr magneton. The electron-hole pairs created by the precession exist for some lifetime τ before relaxing through lattice scattering. The amount of energy and angular momentum dissipated to the lattice depends on how far from equilibrium the system gets; thus, damping by this mechanism increases linearly with the electron lifetime as seen in Eq. (2). Since the electron lifetime is expected to decrease as the temperature increases, this model predicts that damping diminishes as the temperature is raised.

Because the predicted damping rate is linear in the scattering time, the damping rate cannot be calculated more accurately than the scattering time is known. For this reason it is not possible to make quantitative comparisons between calculations of the breathing Fermi surface and measurements. Further, while the breathing Fermi surface model can explain the dramatic temperature dependence observed in the conductivitylike portion of the data it fails to capture the physics driving the resistivitylike term. This is a significant limitation from a practical perspective because the resistivitylike term dominates damping at room temperature and above and is the only contribution observed in iron [13] and NiFe alloys [26].

Kambersky's torque-correlation model predicts

$$\lambda = \frac{g^2\mu_B^2}{\hbar}\sum_{n,m}\int\frac{dk^3}{(2\pi)^3}|\Gamma^-_{nm}(k)|^2 W_{nm}(k) \qquad (3)$$

and we will show that it both incorporates the physics of the breathing Fermi surface model and also accounts for the resistivitylike terms. The matrix elements $\Gamma^-_{nm}(k) = \langle n,k|[\sigma^-, H_{\mathrm{so}}]|m,k\rangle$ measure transitions between states in bands n and m induced by the spin-orbit torque. These transitions conserve wave vector k because they describe the annihilation of a uniform precession magnon, which carries no linear momentum. The nature of these scattering events, which are weighted by the spectral overlap $W_{nm}(k) = (1/\pi)\int d\omega_1\,\eta(\omega_1)A_{nk}(\omega_1)A_{mk}(\omega_1)$, will be discussed in more detail below. The electron spectral functions A_{nk} are Lorentzians centered around the band energies ϵ_{nk} and broadened by interactions with the lattice. The width of the spectral function $\hbar/\tau$ provides a phenomenological account for the role of electron-lattice scattering in the damping process. The η function is the same as in Eq. (2) and enforces the requirement of spectral overlap at the Fermi level.

Equation (3) captures two different types of scattering events: scattering within a single band, $m = n$, for which the initial and final states are the same, and scattering between two different bands, $m \neq n$. As explained in [17] the overlap of the spectral functions is proportional (inverse) to the electron scattering time for intraband (interband) scattering. From this observation the qualitative conclusion is made that the intraband contributions match the conductivitylike terms while the interband contributions give the resistivitylike terms. Evaluation of Eq. (3) is more computationally intensive than that of the breathing Fermi surface model and until now only a few estimates for Ni and Fe have been made [19].

We have performed first-principles calculations of the torque-correlation model Eq. (3) with realistic band structures for Fe, Co, and Ni. Prior to evaluating Eq. (3) the eigenstates and energies of each metal were found using the linear augmented plane wave method [27] in the local spin density approximation [28–30]. Details of the calculations for these materials are described in [31]. The exchange field was fixed in the chosen equilibrium magnetization direction. Calculations of Eq. (3) presented in this Letter are converged to within a standard deviation of 3%, which required sampling $(160)^3$ k points for Fe, $(120)^3$ for Ni, and $(100)^2$ k points in the basal plane by 57 along the c axis for Co. Electron-lattice interactions were treated phenomenologically as a broadening of the spectral functions. The Fermi distribution was smeared with an artificial temperature. Results did not vary significantly with reasonable choices of this temperature since the broadening of the Fermi distribution was considerably less than that of the bands. The damping rate was calculated for a range of scattering rates (spectral widths) just as damping has been measured over a range of temperatures.

The results of these calculations are presented in Fig. 1 and are decomposed into the intraband and interband terms. The downward sloping line in Fig. 1 represents the intraband contribution to damping. Damping constants were recently calculated using the breathing Fermi surface model [12,21] by evaluating the derivative of the electronic energy with respect to the spin direction according to Eq. (2). The results of the breathing Fermi surface prediction are indistinguishable from the intraband terms of the present calculation even though the computational approaches differed significantly; the agreement is quantified in Table I.

The breathing Fermi surface model could not be quantitatively compared to the experimental results because the temperature dependence of the scattering rate has not been determined sufficiently accurately. While the present calculations also require knowledge of the scattering rate to determine the damping rate, the nonmonotonic dependence of damping on the scattering rate produces a unique minimum damping rate. In the same manner that the calculated curves of Fig. 1 have a minimum with respect

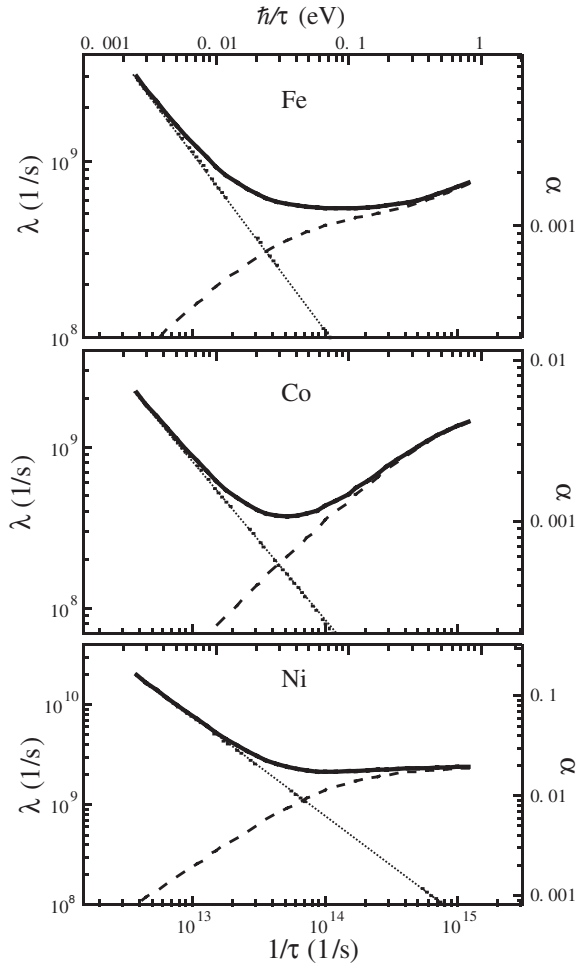

FIG. 1. Calculated Landau-Lifshitz damping constant for Fe, Co, and Ni. Thick solid curves give the total damping parameter while dotted curves give the intraband and dashed lines the interband contributions. Values for λ are given in SI units. The right axis is the equivalent Gilbert damping parameter and the top axis is the full width half maximum of the electron spectral functions.

to scattering rate, the measured damping curves exhibit minima with respect to temperature. Whatever the relation between temperature and scattering rate, the calculated minima may be compared directly and quantitatively to the measured minima. Table I makes this comparison. The agreement between measured and calculated values shows that the torque-correlation model accounts for the dominant contribution to damping in these systems.

Our calculated values are smaller than the measured values. Using measured g values instead of setting $g = 2$ would increase our results by a factor of $(g/2)^2$, or about 10% for Fe and 20% for Co and Ni. Other possible reasons for the difference include a simplified treatment of electron-lattice scattering in which the scattering rates for all states were assumed equal, errors associated with using wave functions found from the mean-field local spin density approximation, and numerical convergence (discussed above). Additionally, the extraction of damping rates from the measured linewidths remains challenging for Fe and particularly for Co. Other damping mechanisms may also make small contributions [22–24].

Since the manipulations involved with the equation of motion techniques employed in deriving Eq. (3) obscure the underlying physics we now discuss the two scattering processes and connect the intraband terms to the breathing Fermi surface model. The intraband terms in Eq. (3) describe scattering from one state to itself by the torque operator, which is similar to a spin-flip operator. A spin-flip operation between some state and itself is only nonzero because the spin-orbit interaction mixes small amounts of the opposite spin direction into each state. Since the initial and final states are the same, the operation is naturally spin conserving. The matrix elements do not describe a real transition, but rather provide a measure of the energy of the electron-hole pairs that are generated as the spin direction changes. The electron-hole pairs are subsequently annihilated by a real electron-lattice scattering event.

To connect the derivatives $\partial\epsilon/\partial\theta$ in Eq. (2) and the torque matrix elements in Eq. (3) we imagine first pointing the magnetization in some direction $\hat{z}$. The only energy that changes with the magnetization direction is the spin-orbit energy H_{so}. As the spin of a single-particle state $|\rangle$ rotates along $\hat{\theta}$ about $\hat{x}$ its spin-orbit energy is given by $\epsilon(\theta) = \langle|e^{i\sigma_x\theta}H_{\mathrm{so}}e^{-i\sigma_x\theta}|\rangle$. The derivative with respect to θ is $\partial\epsilon(\theta)/\partial\theta = i\langle|e^{i\sigma_x\theta}[\sigma_x, H_{\mathrm{so}}]e^{-i\sigma_x\theta}|\rangle$. Evaluating this derivative at the pole ($\theta = 0$) gives $\partial\epsilon/\partial\theta = i\langle|[\sigma_x, H_{\mathrm{so}}]|\rangle$. Similarly, rotating the spin along $\hat{\theta}$ about $\hat{y}$ leads to

TABLE I. Calculated and measured [13] damping parameters. Values for λ are reported in 10^9 s^{-1} while those for α are dimensionless. Values in the first four columns indicate minima of the calculated or measured curves. The last two columns list calculated damping due to the intraband contribution from Eq. (3) and from the breathing Fermi surface model [12], respectively. Values for λ/τ are given in 10^{22} s^{-2}. Published numbers from [12,13] have been multiplied by 4π to convert from the cgs unit system to SI.

	α_{calc}	λ_{calc}	λ_{meas}	$\lambda_{\mathrm{calc}}/\lambda_{\mathrm{meas}}$	$(\lambda/\tau)_{\mathrm{intra}}$	$(\lambda/\tau)_{\mathrm{BFS}}$
bcc Fe ⟨001⟩	0.0013	0.54	0.88	0.61	1.01	0.968
bcc Fe ⟨111⟩	0.0013	0.54	⋯	⋯	1.35	1.29
hcp Co ⟨0001⟩	0.0011	0.37	0.9	0.41	0.786	0.704
fcc Ni ⟨111⟩	0.017	2.1	2.9	0.72	6.67	6.66
fcc Ni ⟨001⟩	0.018	2.2	⋯	⋯	8.61	8.42

$\partial\epsilon/\partial\theta = i\langle|[\sigma_y, H_{so}]|\rangle$. The torque matrix elements in Eq. (3) are $\Gamma^- = \langle|[\sigma^-, H_{so}]|\rangle = \langle|[\sigma_x, H_{so}]|\rangle - i\langle|[\sigma_y, H_{so}]|\rangle$. Using the relations between the commutators and derivatives just found the torque is $\Gamma^- = -i(\partial\epsilon/\partial\theta)_x - (\partial\epsilon/\partial\theta)_y$, where the subscripts indicate the rotation axis. Squaring the torque matrix elements gives $|\Gamma^-|^2 = (\partial\epsilon/\partial\theta)_x^2 + (\partial\epsilon/\partial\theta)_y^2$. For high symmetry directions $(\partial\epsilon/\partial\theta)_x = (\partial\epsilon/\partial\theta)_y$ and we deduce $|\Gamma^-|^2 = 2(\partial\epsilon/\partial\theta)^2$ demonstrating that the intraband terms of the torque-correlation model describe the same physics as the breathing Fermi surface.

The monotonically increasing curves in Fig. 1 indicate the interband contribution to damping. Uniform mode magnons, which have negligible energy, may induce quasielastic transitions between states with different energies. This occurs when lattice scattering broadens bands sufficiently so that they overlap at the Fermi level. These wave vector conserving transitions, which are driven by the precessing exchange field, occur primarily between states with significantly different spin character. The process may roughly be thought of as the decay of a uniform precession magnon into a single electron spin-flip excitation. These events occur more frequently as the band overlaps increase. For this reason the interband terms, which qualitatively match the resistivitylike contributions in the experimental data, dominate damping at room temperature and above.

We have calculated the Landau-Lifshitz damping parameter for the itinerant ferromagnets Fe, Co, and Ni as a function of the electron-lattice scattering rate. The intraband and interband components match qualitatively to conductivity and resistivitylike terms observed in FMR measurements. A quantitative comparison was made between the minimal damping rates calculated as a function of scattering rate and measured with respect to temperature. This comparison demonstrates that our calculations account for the dominant contribution to damping in these systems and identify the primary damping mechanism. At room temperature and above, damping occurs overwhelmingly through the interband transitions. The contribution of these terms depends in part on the band gap spectrum around the Fermi level, which could be adjusted through doping.

K. G. and Y. U. I. acknowledge the support of the Office of Naval Research through Grant No. N00014-03-1-0692 and through Grant No. N00014-06-1-1016. We would like to thank R. D. McMichael and T. J. Silva for valuable discussions.

[1] L. Landau and E. Lifshitz, Phys. Z. Sowjetunion **8**, 153 (1935).
[2] T. L. Gilbert, Armour Research Foundation Project No. A059, 1956 (unpublished).
[3] T. L. Gilbert, IEEE Trans. Magn. **40**, 3443 (2004).
[4] D. J. Twisselmann and R. D. McMichael, J. Appl. Phys. **93**, 6903 (2003).
[5] T. Gerrits, J. Hohlfeld, O. Gielkens, K. J. Veenstra, K. Bal, T. Rasing, and H. A. M. van den Berg, J. Appl. Phys. **89**, 7648 (2001).
[6] W. E. Bailey, L. Cheng, D. J. Keavney, C. C. Kao, E. Vescovo, and D. A. Arena, Phys. Rev. B **70**, 172403 (2004).
[7] I. N. Krivorotov, D. V. Berkov, N. L. Gorn, N. C. Emley, J. C. Sankey, D. C. Ralph, and R. A. Buhrman, arXiv:cond-mat/0703458 [Phys. Rev. B (to be published)].
[8] M. D. Stiles and J. Miltat, *Spin Dynamics in Confined Magnetic Structures III* (Springer, New York, 2006).
[9] J. O. Rantschler, R. D. McMichael, A. Castiello, A. J. Shapiro, W. F. Egelhoff, B. B. Maranville, D. Pulugurtha, A. P. Chen, and L. M. Conners, J. Appl. Phys. **101**, 033911 (2007).
[10] W. Bailey, P. Kabos, F. Mancoff, and S. Russek, IEEE Trans. Magn. **37**, 1749 (2001).
[11] C. Scheck, L. Cheng, I. Barsukov, Z. Frait, and W. E. Bailey, Phys. Rev. Lett. **98**, 117601 (2007).
[12] D. Steiauf and M. Fähnle, Phys. Rev. B **72**, 064450 (2005).
[13] S. M. Bhagat and P. Lubitz, Phys. Rev. B **10**, 179 (1974).
[14] B. Heinrich, D. Fraitová, and V. Kamberský, Phys. Status Solidi **23**, 501 (1967).
[15] B. Heinrich, D. J. Meredith, and J. F. Cochran, J. Appl. Phys. **50**, 7726 (1979).
[16] J. F. Cochran and B. Heinrich, IEEE Trans. Magn. **16**, 660 (1980).
[17] V. Kamberský, Czechoslovak Journal of Physics, Section B **26**, 1366 (1976).
[18] V. Kamberský, Can. J. Phys. **48**, 2906 (1970).
[19] V. Kamberský, Czechoslovak Journal of Physics, Section B **34**, 1111 (1984).
[20] V. Korenman and R. E. Prange, Phys. Rev. B **6**, 2769 (1972).
[21] J. Kuneš and V. Kamberský, Phys. Rev. B **65**, 212411 (2002).
[22] R. D. McMichael and A. Kunz, J. Appl. Phys. **91**, 8650 (2002).
[23] E. Rossi, O. G. Heinonen, and A. H. MacDonald, Phys. Rev. B **72**, 174412 (2005).
[24] Y. Tserkovnyak, G. A. Fiete, and B. I. Halperin, Appl. Phys. Lett. **84**, 5234 (2004).
[25] B. Heinrich, *Ultrathin Magnetic Structures III* (Springer, New York, 2005).
[26] S. Ingvarsson, L. Ritchie, X. Y. Liu, G. Xiao, J. C. Slonczewski, P. L. Trouilloud, and R. H. Koch, Phys. Rev. B **66**, 214416 (2002).
[27] L. F. Mattheiss and D. R. Hamann, Phys. Rev. B **33**, 823 (1986).
[28] P. Hohenberg and W. Kohn, Phys. Rev. **136**, B864 (1964).
[29] W. Kohn and L. J. Sham, Phys. Rev. **140**, A1133 (1965).
[30] U. von Barth and L. Hedin, J. Phys. C **5**, 1629 (1972).
[31] M. D. Stiles, S. V. Halilov, R. A. Hyman, and A. Zangwill, Phys. Rev. B **64**, 104430 (2001).